

An anti-infective peptide that selectively modulates the innate immune response

Monisha G Scott¹, Edie Dullaghan^{1,4}, Neeloffer Mookherjee^{2,4}, Natalie Glavas¹, Matthew Waldbrook², Annick Thompson¹, Aikun Wang¹, Ken Lee¹, Silvana Doria², Pam Hamill², Jie Jessie Yu², Yuexin Li², Oreola Donini¹, M Marta Guarna¹, B Brett Finlay³, John R North¹ & Robert E W Hancock²

We show that an innate defense-regulator peptide (IDR-1) was protective in mouse models of infection with important Gram-positive and Gram-negative pathogens, including methicillin-resistant *Staphylococcus aureus*, vancomycin-resistant *Enterococcus* and *Salmonella enterica* serovar Typhimurium. When given from 48 h before to 6 h after infection, the peptide was effective by both local and systemic administration. Because protection by IDR-1 was prevented by *in vivo* depletion of monocytes and macrophages, but not neutrophils or B- and T-lymphocytes, we conclude that monocytes and macrophages are key effector cells. IDR-1 was not directly antimicrobial: gene and protein expression analysis in human and mouse monocytes and macrophages indicated that IDR-1, acting through mitogen-activated protein kinase and other signaling pathways, enhanced the levels of monocyte chemokines while reducing pro-inflammatory cytokine responses. To our knowledge, an innate defense regulator that counters infection by selective modulation of innate immunity without obvious toxicities has not been reported previously.

The discovery of antibiotics has been one of the great achievements of modern medicine¹, but their excessive use has selected for resistant bacteria. The proportion of infections due to multiply resistant organisms, such as methicillin-resistant *Staphylococcus aureus* (MRSA) and vancomycin-resistant *Enterococcus* (VRE), continues to increase. At the same time there has been a decline in the development of new antibacterial therapies². Novel approaches to anti-infective therapy, including immunomodulatory therapy, are under investigation. Modulation of innate immunity is an attractive approach^{3–5} as it has many features that are consistent with antibiotic therapies but potentially has broader applications and may avoid or reduce concerns of bacterial resistance.

The innate response is the first line of defense against infectious agents^{6–8}. It is an interactive network of cellular and molecular systems responsible for recognizing and eradicating pathogens, and involves a variety of signaling pathways that trigger the rapid deployment of a wide spectrum of biological responses. Foreign molecules, which are present on microbes but not on host cells, are discriminated from self through pathogen-associated signature molecules, including lipopolysaccharide (LPS). Innate defense responses are 'triggered' in part by the binding of these pathogen-associated signature molecules to pattern-recognition receptors, including Toll-like receptors (TLRs). Within minutes to hours, a broad, relatively nonspecific, innate immune response is activated. A major component of this response involves TLR-initiated pathways that culminate in the translocation of NFκB and other transcription factors. Local inflammation plays an

important role in the early response to infection. Numerous cells and molecules, including neutrophils, monocytes, macrophages, complement, cytokines, chemokines and host defense proteins and peptides with antimicrobial properties are marshaled rapidly in a complex and highly orchestrated response to infection. These responses usually kill moderate loads of incoming pathogens effectively and prevent or clear infection. However, the excessive or prolonged triggering of inflammation comes at a potential detriment, as sepsis can be triggered causing massive damage and even death^{5–7}.

Recently it has been demonstrated that natural host defense peptides trigger a range of immunomodulatory responses^{3,9,10}. Of particular interest is their ability to moderate TLR-mediated responses stimulated by pathogen-associated signature molecules^{10,11} and to protect against lethal endotoxemia and infections in animal models^{3,10}. Development of natural host defense peptides has been problematic owing to detrimental activities, such as the induction of toxicities, including mast cell degranulation and apoptosis^{12,13}.

Here we show that IDR-1 was protective in a broad range of *in vivo* infection models by local and systemic administration. IDR-1 was not directly antimicrobial *in vitro* and acted instead on the host innate immune response. We provide evidence that IDR-1 activated several signaling pathways, stimulated the activation of downstream transcription factors like C/EBP and sustained or enhanced the levels of infection-clearing chemokines, while suppressing the levels of pathogen-associated signature molecule/LPS-stimulated pro-inflammatory cytokines such as tumor necrosis factor (TNF)-α without displaying

¹Inimex Pharmaceuticals Inc., 3650 Westbrook Mall, Vancouver, British Columbia, Canada V6S 2L2. ²Centre for Microbial Diseases and Immunity Research and ³Michael Smith Laboratories, 2259 Lower Mall Research Station, University of British Columbia, Vancouver, British Columbia, Canada, V6T 1Z4. ⁴These authors contributed equally to this work. Correspondence should be addressed to R.E.W.H. (bob@cmdr.ubc.ca).

Received 16 January; accepted 16 February; published online 25 March 2007; doi:10.1038/nbt1288

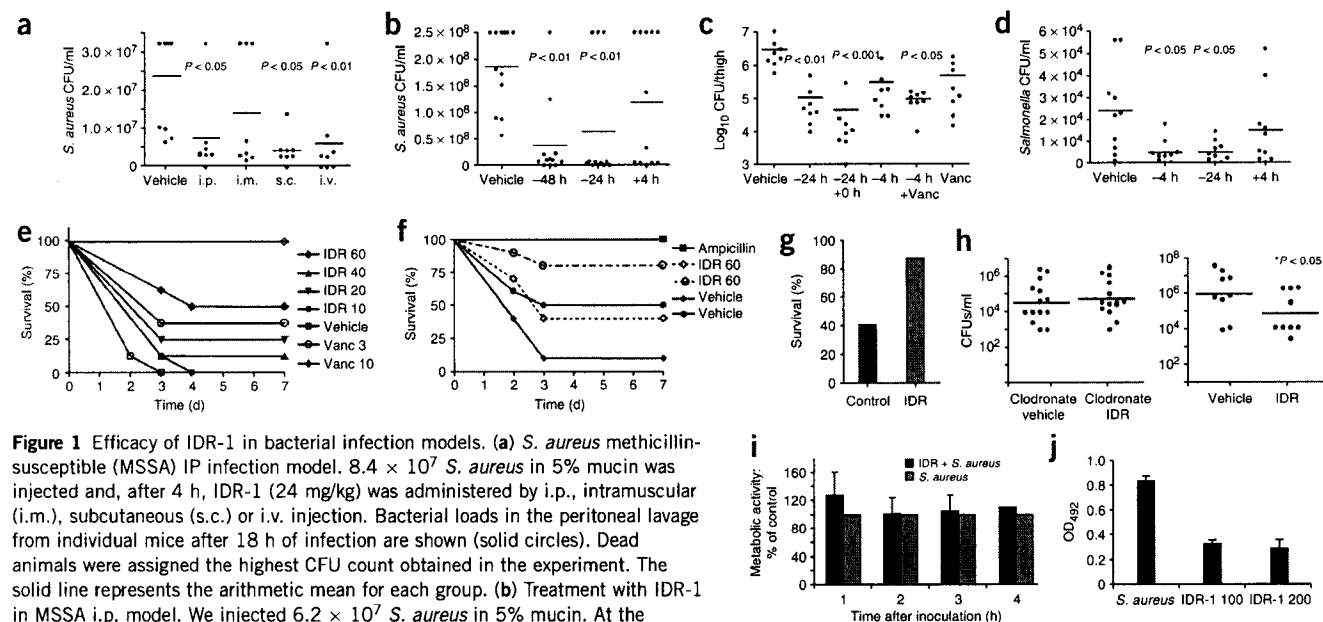


Figure 1 Efficacy of IDR-1 in bacterial infection models. (a) *S. aureus* methicillin-susceptible (MSSA) IP infection model. 8.4×10^7 *S. aureus* in 5% mucin was injected and, after 4 h, IDR-1 (24 mg/kg) was administered by i.p., intramuscular (i.m.), subcutaneous (s.c.) or i.v. injection. Bacterial loads in the peritoneal lavage from individual mice after 18 h of infection are shown (solid circles). Dead animals were assigned the highest CFU count obtained in the experiment. The solid line represents the arithmetic mean for each group. (b) Treatment with IDR-1 in MSSA i.p. model. We injected 6.2×10^7 *S. aureus* in 5% mucin. At the indicated times before (–) or after (+) bacterial addition, IDR-1 was administered by i.p. injection. Results are shown as described above. (c) Thigh model. *S. aureus* (1.8×10^6) was injected into the right thigh muscle. At the indicated times mice were treated with IDR-1. Mice in the positive control group were given vancomycin (Vanc) subcutaneously at 1, 6 or 24 h after infection. Bacterial loads from individual mice are shown (solid circles). Solid line represents arithmetic mean for each group. (d) *Salmonella enterica* serovar Typhimurium i.p. model. BALB/c mice received IDR-1 (8 mg/kg) 4 or 24 h before (–) or 4 h after (+) by i.p. injection of 2.7×10^5 *S. typhimurium*. Bacterial counts in the spleens of individual mice (solid circles) were assessed 24 h later. The solid line represents the arithmetic mean for each group. (e) Methicillin-resistant *S. aureus* (MRSA) model. CD-1 mice were infected by i.p. injection with 0.9×10^7 CFU/mouse of MRSA. IDR-1 or vehicle was administered by i.p. injection 1 h before and 5 h after and vancomycin was administered subcutaneously at 1 and 5 h after MRSA. Survival was recorded over 7 d. Survival curves were significantly different ($P < 0.001$ by log-rank test). IDR, IDR-1. Vanc, vancomycin. The number following is the amount administered in mg/kg. (f) VRE model. CD-1 mice were infected with VRE by i.p. administration. IDR-1 (open diamond) or vehicle (filled diamond) was administered i.p. 1 h before and 5 h after infection or 24 h before infection (IDR-1, open circle; vehicle, filled circle) with 1.8×10^8 CFU/mouse of VRE. Ampicillin was administered subcutaneously at 1 and 5 h after bacterial challenge. Survival was recorded over 7 d. Survival curves were significantly different ($P < 0.01$ by log-rank test). (g) Neutropenic model. CD-1 mice were rendered neutropenic with cyclophosphamide and then infected i.p. with 2.1×10^8 *S. aureus* and IDR-1 (24 mg/kg) administered 4 h later as described in a. Survival was measured at 24 h after infection and was statistically significantly improved ($P < 0.05$ by log-rank test) in the case of the IDR-1 treated mice. (h) Macrophage/monocyte-deficient animal model. To deplete macrophages/monocytes, CD-1 mice were treated once with liposomal clodronate and after 3 d, mice were given 7×10^7 *S. aureus* i.p., as described in b. IDR-1 (24 mg/kg) or vehicle was administered by i.p. injection 24 h before infection and bacterial counts determined in the peritoneal lavage 24 h after infection. Results are the combination of two experiments (total of 14 mice in the clodronate-treated group and 9 in the other groups), representative of four performed. Non-clodronate-treated animals (right-hand panel served as a control). All *in vivo* experiments reported were repeated from two to >10 times. (i) Lack of direct antibacterial effect. The WST-1 assay was used to assess the effect of IDR-1 on the metabolic activity of *S. aureus*. Growth of bacteria is expressed as the percentage of the no-peptide vehicle control. Bars represent mean \pm s.d. (j) IDR-1 protection of human THP-1 cells. THP-1 cells were infected with *S. aureus* with or without IDR-1 (100, 200 μ g/ml) for 18 h and cell toxicity was measured with the LDH cytotoxicity kit. The values on the y-axis represent the OD₄₉₂ reading from the LDH assay and the changes in the peptide-treated samples were significantly different ($P < 0.01$ using ANOVA followed by Dunnett's multiple comparison *t*-test) from control. The data represent the mean of a minimum of three technical repeats for all biological samples. In protection studies, a peptide with the sequence LLGRVVPVWCK-NH₂ served as a negative control peptide (not shown), failing to give any protection against *S. aureus*-mediated cytotoxicity, as indeed it failed to provide protection in any animal model used.

undesirable toxicities. Altered cell trafficking and cytokine/chemokine levels in animal models indicated that these immunomodulatory mechanisms are operative *in vivo*. Given that IDR-1 acts on the host, it is not expected that bacteria will become resistant, indicating that it will be a valuable complement to current anti-infective therapy.

RESULTS

Activity of IDR-1 in models of infection

Extrapolating from our recent demonstration¹⁴ that small cationic peptides have immunomodulatory properties, we designed a series of peptides with varied length and charge, but containing features incompatible with direct antimicrobial activity. These peptides were screened for their immunomodulatory properties and for efficacy in

an infection model. A 13-amino acid peptide, IDR-1 (KSRIV-PAIPVSL-NH₂), that demonstrated protective ability, with an extended conformation (that is, not helical) and a net charge of +3, was selected for further characterization.

We established a mouse model of aggressive bacterial infection, widely used to assess antibiotic efficacy¹⁵, with *S. aureus*, a major cause of nosocomial infections. IDR-1 was given by different routes after *S. aureus* intraperitoneal (i.p.) challenge. We observed substantial protection (Fig. 1a–c) when the peptide was given either locally by the i.p. injection (at concentrations ranging from 8 to 24 mg/kg) or at distant sites, by subcutaneous or intravenous (i.v.) injection (Fig. 1a). Complete eradication of bacteria was rarely seen in any model, but IDR-1 significantly ($P < 0.05$) decreased bacterial counts and mortality. IDR-1 was given either 24 or 48 h prior (–24 h or –48 h) to or 4 h

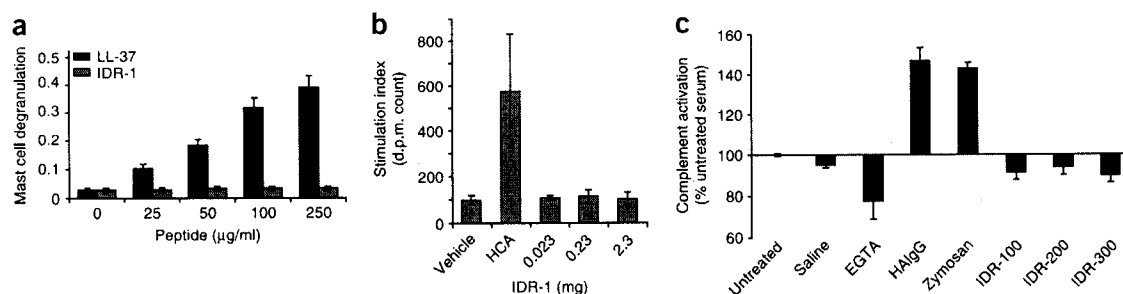


Figure 2 Lack of IDR-1 toxicity. (a) Histamine release from the supernatant of RBL-2H3 mast cells incubated with IDR-1 or LL-37 was determined by the α -phthalaldehyde spectrofluorimetric procedure, and is expressed in units of OD₄₀₅. Results shown are the average of three independent experiments \pm s.d. (b) Lymph node cell proliferation. CBA/J mice (five/group) were administered three doses of peptide (with the highest dose of IDR-1 based on the limit of solubility), hexylcinnamaldehyde (HCA; 50%) or peptide vehicle over 3 consecutive days. On day 6 proliferation of lymph node cells was assessed by the incorporation of ³H-thymidine. The corresponding average incorporation (in d.p.m.) \pm s.d. is shown. (c) Complement activation. Human serum was treated with saline vehicle, EGTA, HAIgG, zymosan and IDR-1 for 1 h; C3a was measured by ELISA. Results shown represent the average percentage values (relative to the saline vehicle) of two independent experiments \pm s.d.

after (+4 h) bacterial challenge, and similar efficacy was demonstrated in all cases (Fig. 1b). Combinations of subeffective doses of both IDR-1 and the antibiotic cefepime (Maxipime) led to increased protection compared to either agent alone (Supplementary Fig. 1 online, note that IDR-1 was effective 6 h after challenge), indicating the potential to use IDR-1 when antibiotic therapy alone is inadequate. IDR-1 was also effective in a local *S. aureus* thigh infection model when given alone or in combination with a standard antibiotic (Fig. 1c). In addition, IDR-1 was effective in this model when administered in the contralateral thigh (Supplementary Fig. 2 online), providing further evidence that it is effective by nonlocal administration.

Protection was also observed in a *Salmonella enterica* serovar Typhimurium infection, although only pretreatment led to significant protection (Fig. 1d). Common bacterial resistances did not prevent peptide protection, as IDR-1 significantly ($P < 0.05$) lowered lethality in models of MRSA (Fig. 1e) and VRE (Fig. 1f) infection. Neutrophils did not appear important in the action of IDR-1, as neutropenic mice were significantly ($P < 0.05$) protected against *S. aureus* (Fig. 1g). Protection was also demonstrated in *Rag1*^{-/-} mice deficient in B- and T-lymphocytes (Supplementary Fig. 3 online). In contrast, depletion of macrophages and/or monocytes using liposomal clodronate (Bonefos) (Fig. 1h) blocked protection, indicating a pivotal role for these cells in IDR-1-mediated protection. Because IDR-1 is composed of L-amino acids, has a short half-life (<30 min) and no direct antimicrobial activity, and protects animals from bacterial infection by a variety of routes, the peptide likely triggers a protective response rather than acting directly on bacteria.

IDR-1 lacks direct antimicrobial activity

The minimal inhibitory concentration (MIC) for IDR-1 was >128 μ g/ml against *S. aureus* and *Escherichia coli*. Similarly, in time-kill assays, 200 μ g/ml of IDR-1 did not kill these organisms suspended in 10 mM sodium phosphate buffer, pH 7.2 or Mueller Hinton broth growth medium. No alteration of bacterial metabolic activity was detected during the exponential growth phase of *S. aureus* using the tetrazolium salt WST-1 (Fig. 1i). However, intriguingly, IDR-1 was able to stabilize human THP-1 monocytic cells (Fig. 1j) and mouse bone marrow-derived macrophages to the cytotoxic effects of *S. aureus*. A peptide with the sequence LLCRIVPVIPWCK-NH₂ served as a negative control in these studies as it also failed to provide protection in any animal model used.

Lack of toxic side effects of IDR-1 treatment

Single dose acute toxicity studies (24 h) in animals are necessary for pharmaceuticals intended for humans. The maximum tolerable dose is defined as the highest amount of administered substance that does not kill test animals. IDR-1 was tested for acute toxicity by i.v. delivery in female outbred mice. The maximum tolerable dose of IDR-1 by i.v. delivery was between 100 and 125 mg/kg, and IDR-1 was not toxic at substantially higher concentrations via the i.p. route, well above the doses used in the infection models.

Hypersensitivity to IDR-1 was tested in a mast cell degranulation assay and the local lymph node assay. Mast cells mediate immediate hypersensitivity reactions and are involved in nonspecific inflammatory reactions^{12,16}. IDR-1 did not induce mast cell degranulation at any dose tested up to 250 μ g/ml (Fig. 2a), in contrast to human cathelicidin LL-37 (refs. 9–11), a host-defense peptide, (Fig. 2a) in confirmation of previous findings¹². The positive controls calcium ionophore and IgE-antigen conjugate induced 65–85% hexaminidase release.

The local lymph node assay tests epidermal skin contact hypersensitization. In this model, mice were dosed over 3 d by painting the dorsal ear with 2.3, 0.23 or 0.023 mg IDR-1 or a positive control, hexylcinnamaldehyde (HCA; 50%). On day 6 after IDR-1 administration, the proliferation of T cells in the draining lymph node was assessed by injecting ³H-thymidine *in vivo*. IDR-1 did not induce hypersensitivity in this model, unlike HCA (Fig. 2b).

The effect of IDR-1 on complement activation was evaluated by measuring, in human serum, C3a lacking its C-terminal arginine (C3a des-Arg), the stable inactive cleavage product of a key intermediate, C3a, in both the classical and alternative pathways of complement activation. IDR-1 showed no significant effect on complement activation, in contrast to the controls (Fig. 2c).

Mechanism of IDR-1 activity

Studies were undertaken to understand the mechanism by which IDR-1 enhanced the resolution of infection without direct antimicrobial activity (Fig. 3). The ability of IDR-1 to modulate the global gene expression pattern of human monocytes was measured using 21,000-oligonucleotide microarrays. A Venn diagram (Supplementary Fig. 4 online) revealed that there were 566, 836 and 1,012 genes uniquely differentially expressed after 4 h by IDR-1, LPS and the combination of IDR-1 and LPS, respectively. There were considerable differences in

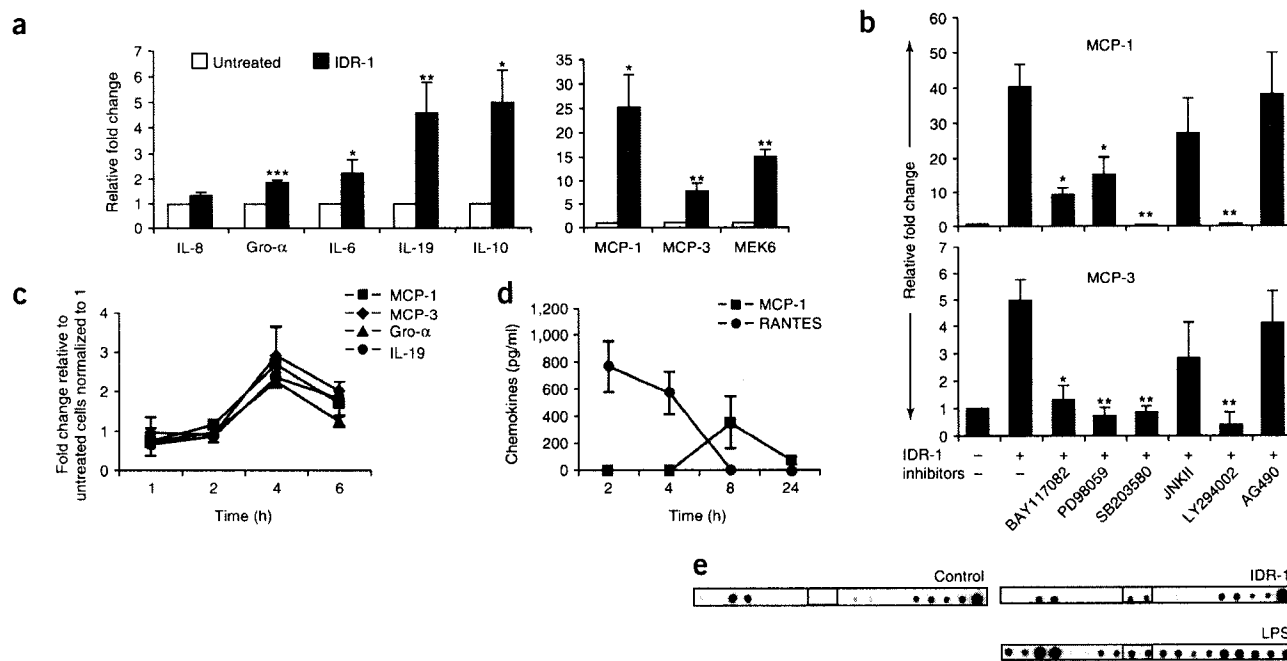


Figure 3 Selective stimulation of innate immunity by IDR-1. (a) Gene expression in response to IDR-1. Human PBMCs¹¹ were stimulated with IDR-1 for 4 h. RNA from CD14⁺ monocytes subsequently isolated was used for qPCR. Fold changes (y-axis) for each gene were normalized to GAPDH and are relative to the gene expression in unstimulated cells (normalized to 1) using the comparative Ct method. Results are the mean \pm s.e.m. from four independent donors (*, $P < 0.05$; **, $P < 0.01$; ***, $P < 0.001$). (b) Effects of specific inhibitors. Human PBMCs were pretreated with specific inhibitors (10 μ M each) for NF κ B (I κ B- α inhibitor BAY117082), ERK1/2 (PD98059), p38 (SB203580), JNK (JNK II-inhibitor), PI3K (LY294002) and JAK-STAT (AG490) pathways for 1 h. Subsequently the cells were stimulated with IDR-1 (200 μ g/ml) for 4 h. RNA isolated from the PBMCs was analyzed for gene expression by real-time quantitative PCR (qPCR). Fold changes (y-axis) for each gene were normalized to GAPDH and are relative to the gene expression in unstimulated cells (normalized to 1) using the comparative Ct method. Results are the mean \pm s.e.m. from three independent donors (*, $P < 0.05$; **, $P < 0.01$). (c) Kinetics of IDR-1-induced responses in human PBMC. Human PBMCs were stimulated with IDR-1 (200 μ g/ml). RNA isolated after 1, 2, 4 and 6 h was analyzed for gene expression by quantitative real time PCR (qPCR). Fold changes (y-axis) for each gene were normalized to GAPDH and are relative to the gene expression in unstimulated cells (normalized to 1) using the comparative Ct method. (d) Kinetics of IDR-1 induced responses in human PBMC. Human PBMC were stimulated with IDR-1 (200 μ g/ml). Tissue culture supernatants from human PBMCs stimulated for 2, 4, 8 and 24 h were assessed for MCP-1 and RANTES by ELISA. The results represent IDR-1-induced chemokines in excess of the background levels found in untreated cells. RANTES in particular demonstrated consistently high background production levels (~ 700 pg/ml) in these cells. Results are the mean \pm standard error from three independent donors. (e) Activation of transcription factors. Nuclear extracts (6 μ g) were isolated from bone marrow-derived mouse macrophages, treated with IDR-1 or LPS for 60 min, and tested for transcription factor activity using transcription factor arrays with the consensus-binding sequences for different transcription factors spotted in duplicate. From left to right: AP-1, AP-2, ARE, Brn-3, C/EBP (boxed), CBF, CDP, c-MyB, AP-1 (3 \times higher probe concentration) and control (single spot). Results are representative of two experiments.

the genes induced by these three sets of stimuli, but there was also overlap in that 255 genes responded both to IDR-1 and to LPS, a TLR4 agonist that stimulates innate immunity. Of the genes stimulated by IDR-1 alone, we noted several transcription factors, including STAT1 and several zinc finger and Hox transcription factors, adhesion molecules such as ICAM, NCAM and integrin- α , and genes involved in actin polymerization and cytoskeletal remodeling (Supplementary Table 1 online).

We examined a number of genes using real-time quantitative PCR (qPCR) (Fig. 3a); in particular, a dual-specificity kinase MEK6 (part of the p38 mitogen-activated protein kinase (MAPK) pathway) and monocyte-chemotactic-protein (MCP) chemokines MCP-3/CCL7 and MCP-1/CCL2 were highly upregulated; cytokines of the interleukin (IL)-10 family (e.g., IL-10 and IL-19) were upregulated about fivefold; whereas IL-6 and chemokine Gro- α /CXCL1 were upregulated about twofold. To investigate the kinetics of chemokine induction in human peripheral blood mononuclear cells (PBMCs), we examined the induction of several genes and demonstrated that expression was time dependent in human PBMCs with a peak transcriptional

response at 4 h after addition (Fig. 3c,d), and, for example, MCP-1 induction was concentration-dependent, increasing over the entire range of concentrations from 50 to 500 μ g/ml.

To investigate the mechanism whereby MCP-1 and MCP-3 were upregulated by IDR-1, we used specific inhibitors of key pathways involved in innate immunity. Human PBMCs were pretreated with various inhibitors, and responses induced by IDR-1 were analyzed. Inhibition of degradation of I κ B- α (which releases NF κ B into the nucleus), the MAP kinases p38 or Erk1/2 and the phosphatidylinositol-3-kinase (PI3K) pathway all blocked IDR-1-mediated induction of MCP-1 and MCP-3 mRNA, whereas inhibitors of the JNK and JAK-STAT pathways had no significant effect (Fig. 3b).

In addition, studies at the protein level profiled cytokine and chemokine changes in supernatants of IDR-1-treated cells. Several chemokines were increased in response to IDR-1 treatment of PBMCs (Fig. 3d) and human monocytic THP-1 cells (Supplementary Fig. 5 online; e.g., IDR-1-treated cells produced $3,200 \pm 129$ pg/ml of cytokine IP-10 compared to 180 ± 5 pg/ml for controls).

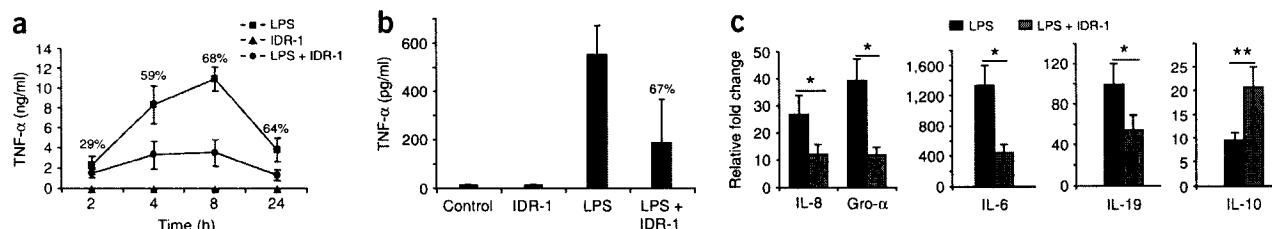


Figure 4 Modulation of LPS-stimulated pro-inflammatory effects. **(a)** Kinetics of anti-endotoxin activity of IDR-1. Human PBMCs were stimulated with LPS (2 ng/ml) in the presence and absence of IDR-1 (200 μg/ml) for 2, 4, 8 and 24 h and supernatants were assessed for TNF-α by ELISA. The cells were pretreated with IDR-1 for 45 min before LPS stimulation. Results show percent inhibition of LPS-induced TNF-α by IDR-1. Results are mean ± s.e.m. from three independent donors and the average percent inhibition ($P < 0.05$ by Student's t -test) is included above each time point. **(b)** Suppression of LPS-induced TNF-α in mouse macrophages. Mouse BMDM were incubated with IDR-1 (200 μg/ml) 45 min before the addition of 2 ng/ml *E. coli* LPS or vehicle control. TNF-α secretion was measured by ELISA after a 17 h incubation. Results are one experiment representative of three performed showing the mean ± s.d. of three replicates, demonstrating significantly lower ($P < 0.05$ by ANOVA) TNF-α production in cells treated with both LPS and IDR-1 compared to cells treated with LPS alone. **(c)** Influence of IDR-1 on LPS-induced gene expression. RNA isolated from CD14⁺ monocytes after 4 h incubation with 2 ng/ml LPS, with or without 200 μg/ml IDR-1, was analyzed by qPCR. Fold changes (y-axis) for each gene were normalized to GAPDH and are relative to the gene expression in unstimulated cells (normalized to 1) using the comparative Ct method. Results are the mean ± s.d. from four independent donors (*, $P < 0.05$; **, $P < 0.01$).

To further understand IDR-1 regulation of chemokines, we used a transcription factor array, revealing that after 1 h, IDR-1, like LPS, increased the appearance of CCAAT/enhancer binding protein (C/EBP proteins) in the nucleus (Fig. 3e) of mouse bone marrow-derived macrophages. The increase in C/EBP was subsequently confirmed by enzyme-linked immunosorbent assay (ELISA) (Supplementary Fig. 5) and similar trends were observed for C/EBP and cAMP-responsive-elements binding-protein in human THP-1 cells. C/EBP, downstream of p38 and ERK1/2 (refs. 17,18), plays a fundamental role in regulating activated macrophage functions, and is involved in control of RANTES, MCP-1 and MCP-3 expression^{19–21}, supporting the hypothesis that IDR-1 induces chemokine changes in part by modulating transcription factor activity and through signaling

pathways such as p38 and ERK1/2. IDR-1 treatment led to a transient increase (peaking at 15–30 min) in NFκB subunit p50 in the nucleus of monocytes, consistent with the ability of an inhibitor of IκB degradation to inhibit chemokine induction (Fig. 3b), in contrast to LPS, which resulted in more sustained NFκB activation (Supplementary Fig. 6 online).

IDR-1 regulates inflammation pathways

Because IDR-1 can upregulate elements of innate immunity such as chemokines, we determined whether it had the potential to cause harmful inflammation by assessing its impact on LPS-induced TNF-α production in primary human and mouse cells. IDR-1 did not increase secretion of TNF-α itself, and reduced LPS-induced TNF-α

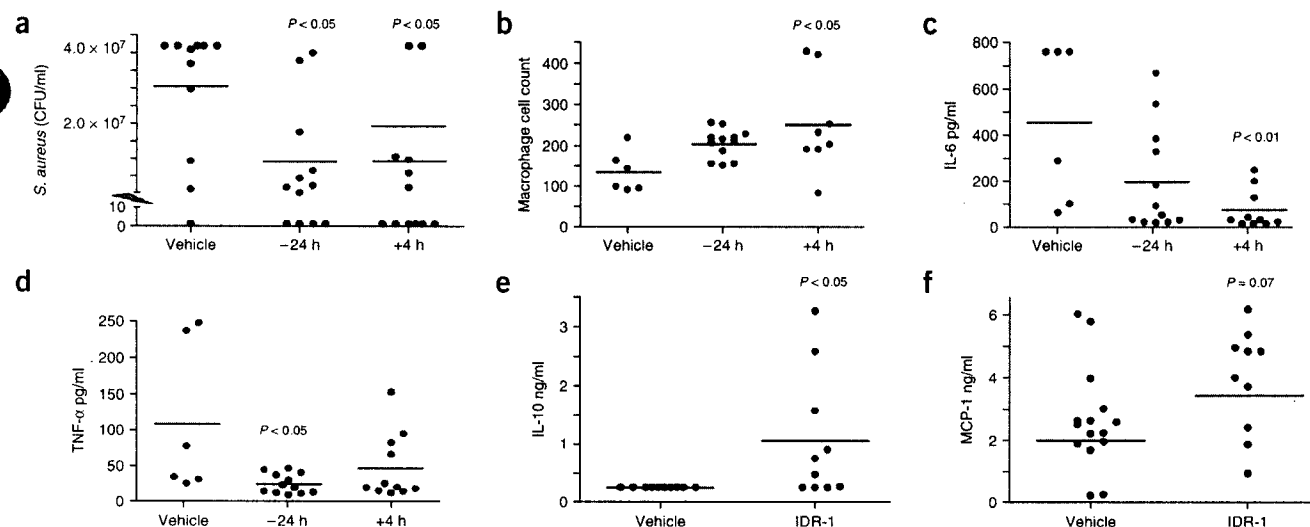


Figure 5 Confirmation of IDR-1 mechanism *in vivo*. **(a–d)** Mice were given i.p. injections of *S. aureus* in 5% mucin. Either 24 h before infection or 4 h after, IDR-1 at 24 mg/kg was injected. Mice were killed 18 h later and the peritoneal lavage fluid was assessed for bacterial load **(a)**, TNF-α by ELISA **(b)**, IL-6 by ELISA **(c)** and cell counts by staining lavage fluid and histochemical analysis of differential cell counts **(d)**. **(e,f)** Mice were given i.p. injections of 7×10^7 *S. aureus* in 5% mucin and IDR-1 at 24 mg/kg was injected i.p. at 24 h before infection. Mice were killed 3 h later, blood collected and the plasma assessed for IL-10 by ELISA **(e)**, and MCP-1 by ELISA **(f)**. For all subgraphs, data from individual mice are shown and solid line represents the arithmetic mean for each group; for each subgraph the mean of the peptide treated mouse values was significantly different from the means of the control mice ($P < 0.05$) except MCP-1 ($P = 0.7$, all by ANOVA with pairwise comparisons).

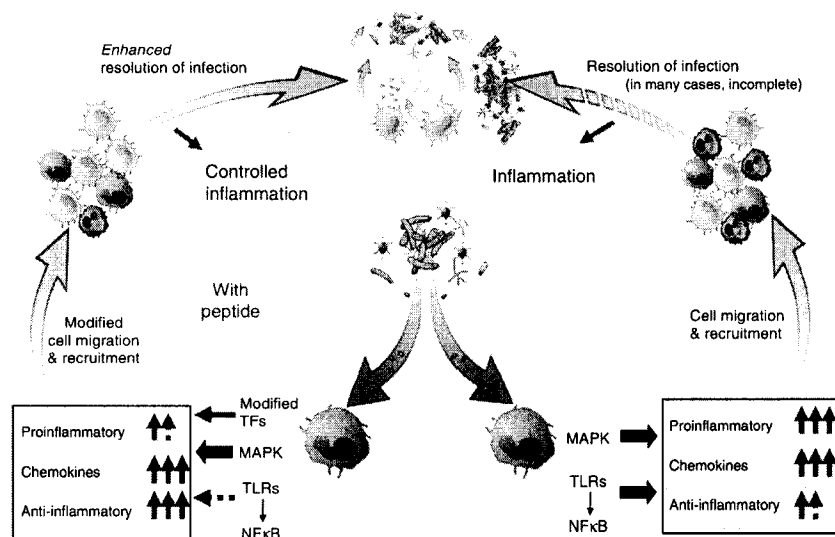


Figure 6 Proposed mechanism of action of IDR-1. Under normal conditions (right-hand side of diagram), the innate immune response is activated by bacterial signature molecules, leading to the activation of the TLR→NFκB and MAP kinase pathways and others. This results in a rapid proinflammatory response which includes the upregulation of pro-inflammatory cytokines, such as TNF-α, and a variety of chemokines, as well as a more moderate anti-inflammatory response that eventually dampens down the pro-inflammatory response. As a result, effectors (including cells and proteins) are recruited to the infection site and assist in resolving infections, complicated by potentially harmful inflammatory reactions. In the presence of peptide IDR-1 (left-hand side of diagram), activation of the TLR→NFκB pathway is modified and that of MAP kinase pathways is maintained, whereas other transcription factors play a role such as C/EBP. These IDR-1-dependent alterations result in reduced production of pro-inflammatory cytokines, maintained or in some cases enhanced chemokine production and an enhanced anti-inflammatory response. Recruitment of cells and effector mechanisms are thus altered, particularly the monocyte-to-neutrophil balance, and infections are efficiently controlled without an increase in potentially harmful inflammation (termed here controlled/balanced inflammation).

in human and mouse cells (Fig. 4a,b), consistent with its ability to induce the anti-inflammatory cytokine IL-10. In kinetic studies with human PBMCs (Fig. 4a), LPS-induced TNF-α production peaked at 4–8 h, whereas IDR-1 suppression of TNF-α was similar at 4, 8 and 24 h. Microarray studies (Supplementary Fig. 4 online) indicated that two-thirds of the genes that responded to LPS treatment of monocytes were not upregulated in the presence of IDR-1. In qPCR with RNA isolated from CD14⁺ monocytes, IDR-1 reduced LPS-induced gene expression of IL-8, Gro-α and IL-6 (Fig. 4c). As each of these cytokines was modestly upregulated by IDR-1 in the absence of LPS, these data emphasize that this peptide balances inflammation rather than merely suppressing it. In contrast, LPS-induced gene expression of the anti-inflammatory mediator IL-10 was significantly ($P < 0.05$) increased by IDR-1 (Fig. 4c). IDR-1 did not affect binding of LPS to LPS binding protein (Supplementary Fig. 7 online), confirming that it did not reduce cytokine secretion by directly blocking LPS.

Supportive *in vivo* observations

To confirm the IDR-1-mediated regulation of immune responses in cultured cells, we administered i.p. peptide either 24 h before or 4 h after *S. aureus* challenge, leading to an effective reduction in both bacterial load and infection-associated mortality (Fig. 5a). Treatment also reduced the levels of the pro-inflammatory cytokines IL-6 and TNF-α in the peritoneal fluid (Fig. 5b,c), confirming that IDR-1 did not induce harmful levels of inflammatory mediators and appeared to control inflammation. IDR-1 resulted in no mortality in the –24 h group and 8% mortality in the +4 h group compared to

50% mortality in the untreated group. In addition, IDR-1-treated animals had an increase in monocyte (but not neutrophil) infiltration, consistent with the modulation of chemokine expression (Fig. 5d). Indeed the average ratio of monocytes to neutrophils was 0.9 in infected mice and increased to 2.2 in IDR-1-treated (+4 h) infected mice. Consistent with these observations, in short-term animal model infection experiments, IDR-1, within 3 h, caused a significant ($P < 0.05$) increase in production in the blood of the anti-inflammatory cytokine IL-10 (Fig. 5e) and a modest increase in the levels of the chemokine MCP-1 (Fig. 5f).

DISCUSSION

Drug development efforts focusing on the regulation of the innate defense system have been limited, in part, because of the potential for inducing harmful sepsis responses^{3,4}. Indeed most antibiotics stimulate the release of bacterial pathogen-associated signature molecule components²² and can contribute to the risk of damaging inflammation and sepsis. As a result, pharmaceutical exploitation of the innate immune response (e.g., through administration of TLR agonists⁴) has been limited to circumstances where stimulation of inflammation can be contained or managed through localized or low dosing, for example, in vaccine adjuvant or allergy applications in which the Th1/Th2 balance is manipulated.

We have identified an immune defense regulator, IDR-1, which can selectively modulate innate immune responses, thereby providing prophylaxis or treatment of a broad spectrum of infections, while balancing or controlling the attendant inflammatory response (Fig. 6). *In vivo* data (Figs. 1h, and 5) implicated macrophages and monocytes as important cells in protection. Macrophages have been shown to phagocytose and directly kill bacteria, to deprive bacteria of vital nutrients, to produce cytokines that influence the differentiation state and growth of the macrophages themselves and other immune cells, and to recruit other cells. Our studies indicated that IDR-1 protects monocytes from the cytotoxic action of staphylococci (Fig. 1j). IDR-1 also stimulated a variety of signaling pathways leading to the induction of key chemokines that are likely responsible for monocyte and/or macrophage recruitment to the site of infection^{19–21}. These include RANTES and MCP-1, which by themselves can protect against infection^{23,24}.

Some of the properties of IDR-1 are reminiscent of the activities of host-defense peptides like defensins and LL-37 (refs. 3,9–12,14), which have immunomodulatory activities that have been proposed to mediate protection in animal models¹⁰. Compared to these, IDR-1 was devoid of any antimicrobial activity, even in dilute broth, is much smaller and thus considerably less expensive to manufacture, and lacks the known toxicities of the natural host-defense peptides such as mast cell degranulation (Fig. 2a), complement activation (Fig. 2c) and cytotoxicity/induction of apoptosis (Fig. 1j). Consistent with these similarities and differences to the host defense peptides, there was only a 33.8% overlap, based on microarray data, in the genes expressed

in response to IDR-1 (Supplementary Table 1 online) compared to LL-37 (data not shown).

In animal models, IDR-1 treatment caused a decrease in both TNF- α and IL-6 at the site of infection and an increase in IL-10 in the blood (Fig. 5). This was consistent with the observed decrease in LPS-induced TNF- α and IL-6 (Fig. 4), as both Gram-negative (LPS) and Gram-positive (lipoteichoic acid) signature molecules cause similar upregulation of proinflammatory cytokines that is suppressible by cationic peptides¹¹. Although IDR-1 itself caused a modest, twofold increase in the expression of IL-6, this was far lower than the 1,300-fold increase observed in response to LPS, whereas the combination of IDR-1 and LPS caused a significant ($P < 0.05$) lowering of IL-6 levels compared to LPS alone. The basis for this anti-inflammatory effect may be contributions from several anti-inflammatory mechanisms, including IL-10 (ref. 25), events resulting from C/EBP activation²⁶ and/or upregulation of suppressor-of-cytokine signaling protein, which is downstream of PI3K pathway activation. These actions of IDR-1 enable it to selectively enhance host immune responses to clear infection while maintaining control of inflammation (Fig. 6).

IDR-1 represents a concept in treating infections that should complement the use of antibiotics. The use of peptides like IDR-1 is unlikely to induce resistance as the peptides did not have any direct effect on microbes. Furthermore it was compatible with the use of antibiotics and did not induce any apparent immunotoxicities. Given the prophylactic efficacy of IDR-1, and its inability to engender resistance, appropriate uses for such agents would include situations in which there is a high risk of infection such as in ventilator-associated pneumonia, after major surgeries, catheterization or insertion of other medical devices, and high-dose myelosuppressive chemotherapy. In the latter situation, the ability of the peptides to work in neutropenic animals can be considered a major asset.

METHODS

Peptide. IDR-1 (KSRIVPAIPVSL-NH₂) was synthesized by manual solid-phase synthesis using standard fluorenylmethoxycarbonyl (Fmoc) chemistry protocols. The resin and Fmoc amino acids were purchased from Novabiochem. The peptide was cleaved from the resin using 95% TFA, 2.5% TIPS (triisopropylsilane) and 2.5% water followed by precipitation with diethylether. The peptide was purified by low pressure chromatography using a reversed-phase solid phase (C18 silica gel, Toronto Research Chemicals). The purified peptide was analyzed by reversed-phase high performance liquid chromatography (HPLC). The purity of the peptide was 94% by HPLC. The molecular weight was confirmed by the [M+H]⁺, observed using matrix assisted laser desorption/ionization-time of flight (MALDI-TOF) mass spectroscopy. LPS was either purified from *Pseudomonas aeruginosa* as previously described¹¹ or purchased commercially (*E. coli* O111:B4 LPS).

Cells. Cells were isolated from normal human volunteers in accordance with UBC ethical approval and guidelines as previously described¹¹ (see also Supplementary Methods online). For mouse cells, ICR mice were killed and bone marrow cells were flushed from the femur using a 25-gauge needle with growth medium (RPMI supplemented with 10% FBS and 20% L929 cells conditioned media) at 20 °C. Cells were seeded in 100-mm Petri dishes and nonadherent cells were removed after 2 d. Adherent cells were further cultivated for 3–4 d, after which they were detached using Versene 1:5,000 (Invitrogen) and seeded in 96-well plates at a density of 8×10^4 cells per well. THP-1 (TIB-202) and L929 (CCL-1) cells were purchased from the American Type Culture Collection (ATCC).

Animal models. Experiments using animal models were performed in accordance with UBC animal care ethics approval and guidelines, as per animal care certificate no. A04-0020. *S. aureus* (ATCC 25293) was injected into female CD1 mice. IDR-1 was administered at 2.5 to 24 mg/kg, as described (Figs. 1 and 5). Animals that died during the study were assigned the highest colony forming

unit (CFU) count obtained in the experiment. In the thigh model, female Swiss albino mice were infected with 0.1 ml of *S. aureus* (ATCC 29213) suspension in the right thigh muscle (eight mice/group). At 48 or 24 h before infection or at the time of infection, mice were treated intramuscularly with IDR-1 (100 mg/kg). Bacterial counts from the thigh were done 24 h after infection. For the MRSA (ATCC 33591) and VRE (ATCC 51575) models, ICR males weighing 24 ± 2 g were administered a LD₉₀₋₁₀₀ dose (lethal dose killing 90–100% of mice) bacterial challenge suspended in 0.5 ml brain-heart infusion broth containing 5% mucin by i.p. injection; vehicle is (0.9% NaCl, 10 ml/kg) given by i.p. injection. In the case of VRE, a dose of 1.8×10^8 CFU/mouse was used (10 mice/group). For MRSA the LD₉₀₋₁₀₀ dose used was 0.9×10^7 CFU/mouse (8 mice/group). The vehicle was administered 1 h before inoculum and 5 h after inoculum. Peptide (10–60 mg/kg i.p.) was administered 24 h before or 1 h before inoculum and 5 h after inoculum. Mortality was recorded daily during the following 7 d. For the *Salmonella* model, BALB/c mice were given 1×10^5 *Salmonella enterica* serovar Typhimurium and IDR-1 (8 mg/kg) by i.p. injection. The mice were monitored for 24 h at which point they were killed, the spleen removed, homogenized and resuspended in PBS and plated on Luria Broth agar plates with kanamycin (50 μ g/ml). The plates were incubated overnight at 37 °C and counted for viable bacteria. For the neutropenic model, mice were rendered neutropenic with two doses of cyclophosphamide (200 mg/kg and 150 mg/kg, eight mice/group) and subsequently infected and treated as described for the *S. aureus* i.p. model. The neutropenic status of the mice was verified by blood counts (blood smears). For the clodronate model, macrophages/monocytes were depleted in CD-1 mice by treatment with liposomal clodronate (200 μ g of clodronate, Sigma) and permitted to rest for 3 d, at which time they remained depleted of macrophage or monocytes, as described previously²⁷. Subsequently a protection experiment was performed, essentially as described in Figure 1b above, in that 7×10^7 *S. aureus* were given 24 h after IDR-1 (24 mg/kg) or a vehicle control, and bacterial counts determined in the peritoneal lavage 24 h after the initiation of infection. For acute toxicity studies, mice were observed for 24 h after i.v. delivery of IDR-1. Observations included respiration, movement, hunched abdomen and diarrhea. Mice were killed at the 24 h time point. Vehicle and TFA (present in peptide preparations) groups were included as controls. For the local lymph node assay study, on three consecutive days CBA/J mice (five/group) were administered 25 μ l of peptide (2.3, 0.23 or 0.023 mg), hexylcinnamaldehyde (HCA; 50% in acetone/olive oil (4:1 vol/vol)) or peptide vehicle (50% vol/vol, acetone/saline). On day 6, the proliferation of lymph node cells was assessed by the average incorporation (in d.p.m.) \pm s.d. of ³H-thymidine.

Antimicrobial assays. For the WST assay, *S. aureus* (ATCC 25293) grown in Luria Broth, was diluted in DMEM. IDR-1 was added at a final concentration of 200 μ g/ml. At $T = 0$, 10 μ l/well of WST-1 reagent was added and the plate incubated at 37 °C. At the indicated time points, absorbance was measured at 450 nm. Growth was expressed as the percentage of the no-peptide control. The data represent the mean \pm s.d. A standard MIC assay was also performed with *S. aureus* ATCC 25293 and *E. coli* ATCC 33694. A fixed inoculum of either *S. aureus* or *E. coli* grown in Mueller-Hinton broth medium was seeded into serial dilutions of peptide or, as controls, of the antibiotics erythromycin or polymyxin B prepared in 96-well plates. Bacterial growth was recorded visually after 24 h and the MIC endpoint leading to 80% growth inhibition was recorded. Serial dilutions of compounds were done in Mueller-Hinton broth medium. Conversely logarithmic phase bacteria were resuspended in 10 mM sodium phosphate buffer pH 7.2 and treated with up to 200 μ g/ml of peptide for up to 4 h. For the cell protection assay, THP-1 cells were seeded at a density of 8×10^4 cells/well in a 96-well plate and activated with 0.5 μ g/ml phorbol myristate (PMA). Twenty-four hours after removing the PMA, the cells were infected with *S. aureus* with or without IDR-1 (100, 200 μ g/ml) for 18 h and cell toxicity was measured with the lactate dehydrogenase cytotoxicity kit (absorbance measured at OD₄₉₂).

RBL-2H3 degranulation assay. RBL-2H3 cells (ATCC CRL 2256) were seeded at 2×10^4 cells/well, 16–20 h before treatment. Culture medium was replaced with Tyrodes's buffer containing 10 mM HEPES, 130 mM NaCl, 5 mM KCl, 1.4 mM CaCl₂, 1 mM MgCl₂, 5.6 mM glucose and 0.1% bovine serum albumin. IDR-1, Triton X-100 or LL-37 was incubated for 30 min at 37 °C

and then supernatant was incubated with 4-nitrophenyl-N-acetyl- β -D-glucosaminide substrate for 90 min at 37 °C. Absorbance was measured at 405 nm with a spectrophotometer. The intensity of color formed in the assay is proportional to the amount of β -hexosaminidase released.

Complement assay. Human serum (Bioreclamations Inc.) was treated with saline vehicle, ethylene glycol tetraacetic acid (EGTA) inhibitor (Sigma Z4250) at 0.01 M, classical pathway activator HAIgG (Antibodies Inc.) at 10 mg/ml, zymosan at 0.5 μ g/ml or IDR-1 at 100, 200 and 300 μ g/ml for 1 h at 37 °C/5% CO₂. C3a des-Arg was measured by ELISA (Cedarlane). The average values of two independent experiments \pm s.d. are shown and expressed as percent complement activation relative to the vehicle control.

Transcription factor arrays. Mouse bone marrow-derived macrophages were treated with IDR-1 for 1 h and then lysed. The pellet was resuspended in 150 μ l of buffer (supplied by manufacturer) and vortexed for 10 s and put on ice and shaken for 2–3 h. Sample was centrifuged at 15,000g for 5 min at 4 °C. The supernatant (nuclear extract) was collected and protein concentration measured. The nuclear extract samples (6 μ g) were mixed with probes and hybridized onto TranSignal Protein/DNA Array 1 (Panomics) as per the manufacturers' directions. The blots were analyzed with ImageQuant TL software from Amersham.

Quantitative real-time PCR (qPCR). RNA isolated from monocytes or PBMCs was analyzed for gene expression by qPCR. Fold changes (y -axis) for each gene were normalized to GAPDH and are relative to the gene expression in unstimulated cells (normalized to 1) using the comparative Ct method²⁴. Details including primers can be found in **Supplementary Methods**.

ELISAs. Tissue culture supernatants from human PBMCs stimulated with IDR-1 (200 μ g/ml) for 2, 4, 8 and 24 h were assessed for MCP-1 and RANTES by ELISA (eBiosciences). Human PBMCs or mouse bone marrow-derived macrophages were stimulated with IDR-1 (200 μ g/ml) in the presence or absence of *P. aeruginosa* LPS (2 ng/ml). When the combination was used, the cells were pretreated for 45 min with IDR-1 before addition of *P. aeruginosa* LPS¹¹ for the human studies or *E. coli* O111:B4 LPS (Sigma) for the mouse cells. Secretion of human TNF- α was monitored by capture ELISA after 24 h of stimulation (eBiosciences). Murine TNF- α secretion was measured by ELISA (BD Biosciences) after 17 h stimulation. A human IP-10 ELISA (BD Biosciences) was used as directed to measure IP-10 in THP-1 supernatants.

Data analysis. The significance of the bacterial colony counts from animal studies was analyzed by the Kruskal-Wallis test (overall P value) and the significance of pair-wise comparisons was calculated using Dunn's Multiple Comparison Test. For microarrays, assessment of slide quality, normalization, detection of differential gene expression and statistical analysis was carried out with ArrayPipe (version 1.6), a web-based, semi-automated software specifically designed for processing of microarray data²⁸ (<http://www.pathogenomics.ca/arraypipe>). Details of methods used for microarray analysis can be found in **Supplementary Methods**. qPCR studies used paired t -tests to determine statistical significance.

Accession codes. Array Express: for microarrays, all data have been deposited under accession number E-FPMI-8.

Note: Supplementary information is available on the Nature Biotechnology website.

ACKNOWLEDGMENTS

We gratefully acknowledge financial support from the Foundation for the National Institutes of Health and Canadian Institutes for Health Research through the Grand Challenges in Global Health Initiative, and from Genome BC for the Pathogenomics of Innate Immunity research program. R.E.W.H. is the recipient of a Canada Research Chair. M.G.S. was the recipient of a Natural Sciences and Engineering Research Council Industrial Fellowship. The authors gratefully acknowledge the technical expertise of Reza Falsafi.

COMPETING INTERESTS STATEMENT

The authors declare competing financial interests: details accompany the full-text HTML version of the paper at www.nature.com/naturebiotechnology/.

Published online at <http://www.nature.com/naturebiotechnology>

Reprints and permissions information is available online at <http://npg.nature.com/reprintsandpermissions>

1. Theuretzbacher, U. & Toney, J.H. Nature's clarion call of antibacterial resistance: are we listening? *Curr. Opin. Investigat. Drugs* **7**, 158–166 (2006).
2. Spellberg, B. *et al.* Trends in Antimicrobial Drug Development: Implications for the Future. *Clin. Infect. Dis.* **38**, 1279–1286 (2004).
3. Finlay, B.B. & Hancock, R.E.W. Can innate immunity be enhanced to treat infections? *Nat. Rev. Microbiol.* **2**, 497–504 (2004).
4. National Research Council Treating Infectious Diseases in a Microbial World: Report of Two Workshops. Washington, D.C.: The National Academies Press, (2005).
5. O'Neill, L.A. How Toll-like receptors signal: what we know and what we don't know. *Curr. Opin. Immunol.* **18**, 3–9 (2006).
6. Pasare, C. & Medzhitov, R. Toll-like receptors: linking innate and adaptive immunity. *Adv. Exp. Med. Biol.* **560**, 11–18 (2005).
7. Tosi, M.F. Innate immune responses to infection. *J. Allergy Clin. Immunol.* **116**, 241–249 (2005).
8. Martinon, F. & Tschopp, J. NLRs join TLRs as innate sensors of pathogens. *Trends Immunol.* **26**, 447–454 (2005).
9. Oppenheim, J.J. & Yang, D. Alarmins: chemotactic activators of immune responses. *Curr. Opin. Immunol.* **17**, 359–365 (2005).
10. Bowdish, D.M.E. *et al.* Impact of LL-37 on anti-infective immunity. *J. Leukoc. Biol.* **77**, 451–459 (2005).
11. Mookherjee, N. *et al.* Modulation of the Toll-like receptor-mediated inflammatory response by the endogenous human host defence peptide LL-37. *J. Immunol.* **176**, 2455–2464 (2006).
12. Niyonsaba, F. *et al.* Evaluation of the effects of peptide antibiotics human beta-defensins-1/2 and LL-37 on histamine release and prostaglandin D(2) production from mast cells. *Eur. J. Immunol.* **31**, 1066–1075 (2001).
13. Lau, Y.E. *et al.* Apoptosis of airway epithelial cells: human serum sensitive induction by the cathelicidin LL-37. *Am. J. Respir. Cell Mol. Biol.* **34**, 399–409 (2006).
14. Bowdish, D.M.E., Davidson, D.J., Scott, M.G. & Hancock, R.E.W. Immunomodulatory activities of small host defence peptides. *Antimicrob. Agents Chemother.* **49**, 1727–1732 (2005).
15. Tsuji, M. *et al.* In vivo antibacterial activity of S-3578, a new broad-spectrum cephalosporin: methicillin-resistant *Staphylococcus aureus* and *Pseudomonas aeruginosa* experimental infection models. *Antimicrob. Agents Chemother.* **47**, 2507–2512 (2003).
16. Gehlhar, K. *et al.* Characterization of modified allergen extracts by in vitro beta-hexosaminidase release from rat basophils. *Int. Arch. Allergy Immunol.* **136**, 311–319 (2005).
17. Hanlon, M., Sturgill, T.W. & Sealy, L. ERK2- and p90(Rsk2)-dependent pathways regulate the CCAAT/enhancer-binding protein-beta interaction with serum response factor. *J. Biol. Chem.* **276**, 38449–38456 (2001).
18. Marcinkowska, E. *et al.* Regulation of C/EBPbeta isoforms by MAPK pathways in HL60 cells induced to differentiate by 1,25-dihydroxyvitamin D3. *Exp. Cell Res.* **312**, 2054–2065 (2006).
19. Fessele, S. *et al.* Molecular and in silico characterization of a promoter module and C/EBP element that mediate LPS-induced RANTES/CCL5 expression in monocytic cells. *FASEB J.* **15**, 577–579 (2001).
20. Williams, S.C. *et al.* C/EBP is a myeloid-specific activator of cytokine, chemokine, and macrophage-colony-stimulating factor receptor genes. *J. Biol. Chem.* **273**, 13493–13501 (1998).
21. Kubota, T. *et al.* Representational difference analysis using myeloid cells from C/EBP epsilon deletion mice. *Blood* **96**, 3953–3957 (2000).
22. Prins, J.M. *et al.* Release of tumor necrosis factor and interleukin 6 during antibiotic killing of *Escherichia coli* in whole blood: influence of antibiotic class, antibiotic concentration, and presence of septic serum. *Infect. Immun.* **63**, 2236–2242 (1995).
23. Zisman, D.A. *et al.* Standiford T.J. MCP-1 protects mice in lethal endotoxemia. *J. Clin. Invest.* **99**, 2832–2836 (1997).
24. Cavaillon, J.M., Adib-Conquy, M., Fitting, C., Adrie, C. & Payen, D. Cytokine cascade in sepsis. *Scand. J. Infect. Dis.* **35**, 535–544 (2003).
25. Brenner, S. *et al.* cAMP-induced Interleukin-10 promoter activation depends on CCAAT/enhancer-binding protein expression and monocytic differentiation. *J. Biol. Chem.* **278**, 5597–5604 (2003).
26. Zwergal, A. *et al.* C/EBPbeta blocks p65 phosphorylation and thereby NF- κ B-mediated transcription in TNF-tolerant cells. *J. Immunol.* **177**, 665–672 (2006).
27. Cote, C.K., Van Rooijen, N. & Welkos, S.L. Roles of macrophages and neutrophils in the early host response to *Bacillus anthracis* spores in a mouse model of infection. *Infect. Immun.* **74**, 469–480 (2006).
28. Pfaffl, M.W. A new mathematical model for relative quantification in real-time RT-PCR. *Nucleic Acids Res.* **29**, e45 (2001).
29. Hokamp, K. *et al.* ArrayPipe: a flexible processing pipeline for microarray data. *Nucleic Acids Res.* **32** (Web Server issue), W457–459 (2004).